Journal of Building Engineering 94 (2024) 109967

Contents lists available at ScienceDirect

Journal of Building Engineering

journal homepage: www.elsevier.com/locate/jobe

Microstructure, XRD, and strength performance of ultra-high-performance lightweight concrete containing artificial lightweight fine aggregate and silica fume

Mahdi Rafieizonooz [a, b], Jang-Ho Jay Kim [a, *], Jin-su Kim [a], Jae-Bin Jo [a], Elnaz Khankhaje [b]

[a] School of Civil and Environmental Engineering, Yonsei University, Yonsei-ro 50, Seodaemun-gu, Seoul, 03722, South Korea
[b] Architectural Engineering Program, School of Architecture, Seoul National University of Science and Technology, 232 Gongneung-ro, Gongneung-dong, Nowon-gu, Seoul, 01811, South Korea

ARTICLE INFO

Keywords:
Ultra-high-performance lightweight concrete
Artificial lightweight fine aggregate
Silica fume
SEM
XRD

ABSTRACT

Ultra-high-performance lightweight concrete (UHPLC), a sustainable and environmentally friendly concrete crafted with artificial lightweight aggregates to preserve non-renewable natural resources like river sand, has garnered significant attention due to its exceptional mechanical properties. This study explores the use of artificial lightweight fine aggregate (ALWFA) as a substitute for fine aggregate in UHPLC production, investigating both fresh properties and mechanical performance. Microstructure analysis, utilizing SEM, and crystalline phase evaluation, employing XRD, were also conducted. The study results indicated that due to the irregular shape of ALWA particles with sharp edges, increasing the content of ALWFA led to a reduction in the flowability of UHPLC. Additionally, it was found that increasing the amount of ALWFA as a replacement for fine aggregate negatively affected both the compressive and tensile strength of UHPLC. This reduction in strength can be attributed to the higher porosity and lower intrinsic strength of ALWFA particles, as well as the weaker cohesion between ALWFA particles and the matrix. SEM analysis revealed that elevating the ALWFA content as a replacement for fine aggregate resulted in an increase in both the number and dimensions of voids, which is responsible for the weaker performance of ALWFA concrete. Finally, XRD analysis showed no significant alteration in the crystalline phases as the ALWFA content increased.

1. Introduction

Ultra-high-performance lightweight concrete (UHPLC), a sustainable and eco-friendly concrete made with lightweight aggregates to preserve non-renewable natural resources such as river sand, has attracted extensive attention on account of its outstanding mechanical properties [1]. Based on the existing information, the excessive use of natural aggregates has put a significant strain on the environment [2]. As a result, considerable work has been done to create eco-friendly lightweight aggregates for making concrete. These alternatives aim to conserve natural resources, decrease the need for landfills by utilizing industrial and urban waste products, promote a sustainable construction industry, and reduce the total weight of the structure [3]. Up to now, various types of grain-like solid wastes have been used as alternative aggregates in concrete, e.g., geopolymer [2], fly ash (FA) [4–7], municipal solid wastes [8], recycled aggregates [9,10], biochar [11], waste concrete [12,13], bottom ash (BA) [14–16], steel slag [17,18], plastic waste [19–22]

* Corresponding author.
E-mail address: jjhkim@yonsei.ac.kr (J.-H. Jay Kim).

https://doi.org/10.1016/j.jobe.2024.109967
Received 29 April 2024; Received in revised form 14 June 2024; Accepted 15 June 2024
Available online 17 June 2024

and waste glass [23]. As the study of granular waste materials advances, there is a growing focus on transforming powdered solid wastes into lightweight aggregates with a granular texture [2].

In general, lightweight aggregates are divided into natural lightweight aggregates using natural minerals and artificial lightweight aggregates (ALWA) using industrial wastes such as FA, cinder ash, BA, etc. [24]. Considering the size of the particles, ALWAs themself can be divided into artificial lightweight fine aggregate (ALWFA) and artificial lightweight coarse aggregate (ALACA) [25–28]. Lately, the concrete industry has shown interest in ALWFAs, especially for applications like panels with enhanced insulation and essential structural components such as walls and slabs. This is due to the reduced density of ALWFA concrete, which results in more affordable transportation and easier handling at construction sites [29]. Pre-saturated ALWFAs serve as an internal reservoir, providing additional moisture to facilitate cement hydration [1], which in turn improves the microstructure of the concrete [30].

To investigate the effect of ALWFA on the mechanical performance of UHPLC, Liu et al. [30] conducted a study and found that pretreated ALWFA using normal soaking and vacuum saturation provided internal curing water for progressive hydration, and enhanced the microstructure at the interface of ALWFA and the bulk paste. In another study, the mechanical properties and durability performance of lightweight aggregate concrete (LAC) incorporating silica fume (SF) were investigated by Youm et al. [31]. The authors reported that the durability against chemical attacks for LAC containing SF depended on the composition of the hardened cement pastes in concretes, while the durability against physical attack depended on the types of aggregates. In addition, they reported that the compressive strength of LAC was increased with an increment in the content of SF, while the tensile strength and elastic modulus had nothing to do with the amount of SF regardless of the types of aggregates. Another work [1] evaluated the mechanical and durability performance of LAC incorporating ALWFA, metakaolin, and FA. The authors reported that by increasing the amount of FA as a partial replacement for cement, the compressive strength was reduced leading to a reduction in the final durability. In addition, they believed that the pre-saturated ALWFA can provide extra curing water inside the concrete matrix leading to achieving a higher hydration rate of cement with more hydrates making a denser microstructure.

Jiang et al. [32] explored the design of UHPLC using lightweight aggregates and graphene oxide (GO) through the modified Andreasen and Andersen (MAA) model, aiming to address the high density of ultra-high-performance concrete and enhance its application in high-rise and long-span structures. Based on the results of this work, it was found that incorporating GO into UHPLC improved its flexural strength, compressive strength, elastic modulus, and internal pore structure, with the optimal GO content being 0.06 wt%. In another study [33], an approach to manufacturing UHPLC using shale ceramic sand and air-entraining agent was proposed, revealing that the optimal air-entraining agent proportion of 0.01 % improved specific strength and created a homogeneous void system, despite reductions in elastic modulus, compressive strength, and flexural strength.

Castillo et al. [19] studied the inclusion of artificial aggregate manufactured using plastic waste to develop an LAC mixture. The results of this research indicated that an LAC with appropriate compressive strength can be produced by utilizing plastic aggregates. The effect of ALWFA on the compressive strength of self-compacting concrete was investigated by Ref. [34]. The authors reported that by increasing the content of ALWFA, the compressive strength of LAC was reduced. Jiang et al. [12] developed a study to evaluate the effects of the strength enhancement of ALWFA on concrete properties. They found that appropriate compressive strength can be achieved by utilizing strength-enhanced ALWFA. Another study [5], investigated the effect of FA-based ALWFA on the properties of LAC. The results of this study revealed that an increase in concrete strength was induced by the increase in ash fineness.

The durability of eco-friendly LAC, incorporating ALWFA and various mineral admixtures, was examined against physical and chemical sulfate attack, revealing enhanced sulfate resistance and reduced erosion products due to internal curing, providing a theoretical basis for improving concrete durability under severe environmental conditions [1]. The properties of concrete utilizing ALWA as replacement materials for natural aggregates were examined by Li et al. [25], revealing significant improvements in concrete durability through enhanced resistance to chloride ion penetration, alongside observed reductions in CO2 emissions, energy consumption, and cost, with particular efficacy noted in ALWA incorporating ground granulated blast furnace slag and FA as adhesives without Portland cement.

Drawing insights from the literature review, it becomes apparent that distinct types of ALWFA, each characterized by unique properties, exert diverse influences on the behavior and performance of concrete. On the other hand, the use of substitute materials in the production of UHPLC has emerged as a promising venture for the future. Many companies and construction firms are now closely considering the advantages and viability of ALWFA as an alternative construction material. Hence, there is an urgent need to assess the mechanical properties of lightweight concrete (LAC) with high strength that incorporates ALWFA and to study its microstructure. While it is acknowledged that there may be other manuscripts on similar topics, this study offers distinct contributions to the field. Specifically, it focuses on optimizing the mix design and evaluating the mechanical properties of high-strength ALWFA concrete, targeting specific design parameters such as compressive strength higher than 100 MPa and density lower than 2000 kg/m^3. The selection of a specific type of ALWFA for high-strength LAC was based on prior experimental findings [29,35–37]. Additionally, the combined use of cement, silica fume, and silica powder as binders, along with artificial lightweight fine aggregate in the production of ultra-high-performance lightweight concrete, has not received sufficient attention. Furthermore, this research delves into the microstructure and XRD characteristics of such concrete, which may not have been thoroughly explored in previous studies. Therefore, despite the existence of other manuscripts, this study brings new insights and findings that contribute to advancing sustainable construction practices and filling a critical gap in research.

2. Materials

2.1. Cement

Ultra-high-performance lightweight concrete (UPHLC) was produced using Ordinary Type I Portland cement (OPC) from Asia Cement Co. Ltd. In Seoul, Korea. The specific gravity, soundness, specific surface area, and Loss on ignition of OPC are 3.15, 10 mm, 3200 cm^2/g, and 2.8 %, respectively. The chemical composition of OPC and silica powder (SPW), and silica sand (SS) is provided in Table 1. Upon reviewing the table, it becomes apparent that SS and SPW predominantly consist of SiO_2 (>99 %), with trace amounts of other oxides. In contrast, the primary oxide in OPC is CaO.

2.2. Silica fume (SF)

Silica fume (SF), also known as micro silica, is a byproduct of the production of silicon metal or ferrosilicon alloys. When added to concrete as a partial replacement for cement, SF can have several significant effects on the properties and performance of concrete such as increased strength, improved durability, enhanced impermeability, reduced permeability, and increased cohesion and workability of the concrete [38]. Therefore, in this study, SF (Grade 940U, Elkem, Norway) with a composition of 95 % SiO_2, a Loss on Ignition (LOI) at 950 °C of 1.9 %, and a specific gravity of 2.2 was utilized as a 20 % substitute for OPC.

2.3. Silica sand (SS)

Silica sand (SS) is a key ingredient in the production of concrete, mortar, and various construction materials. It provides strength and durability to the final product. In this study, silica sand (Saeron Co., Ltd., Gangwon-do, Korea) with a diameter of 100–600 μm and density of 2.65 g/cm^3 was used as a fine aggregate. The chemical composition of SS is provided in Table 1. The particle size distribution of SS is illustrated in Fig. 1. It is evident from the graph that the SS particles are smaller than 1 mm in size, enabling them to effectively fill the concrete matrix. This characteristic allows them to actively participate in the hydration process, contributing to the formation of a denser concrete matrix. It should be noted that in this study, saturated surface-dry (SSD) silica sand was utilized. By using SSD aggregates, the aggregates were in a condition where their internal pores were filled with water, but no excess water was present on the surface. To achieve this, the lightweight fine aggregate was first submerged in water for a sufficient period to reach its maximum absorption capacity. After soaking, the aggregates were removed and allowed to dry on a flat surface, with excess surface water removed by patting them with a clean, absorbent cloth. In addition to that, Silica powder (SPW) (S-SIL 10, SAC, Ulsan, Korea), with a diameter of 1–5 μm was used as a fine filler. The chemical composition of SPW is shown in Table 1. Also, in the current work for achieving high compressive strength, reducing the amount of water, and having appropriate workability, a superplasticizer was utilized.

Table 1
Chemical composition of OPC, SPW, and SS.

Chemical Component	SiO_2	Fe_2O_3	Al_2O_3	TiO_2	CaO	MgO	SO_3	MnO	Na_2O	P_2O_5	K_2O
OPC	18.78	2.76	4.72	0.31	65.97	3.14	2.56	0.13	0	0.19	0
SPW	99.59	0.023	0.315	0.042	0.013	0.006	0	0	0.008	0	0.004
SS	99.9	0.0125	0.025	0.049	0.004	0.0041	0	0	0.003	0	0.0021

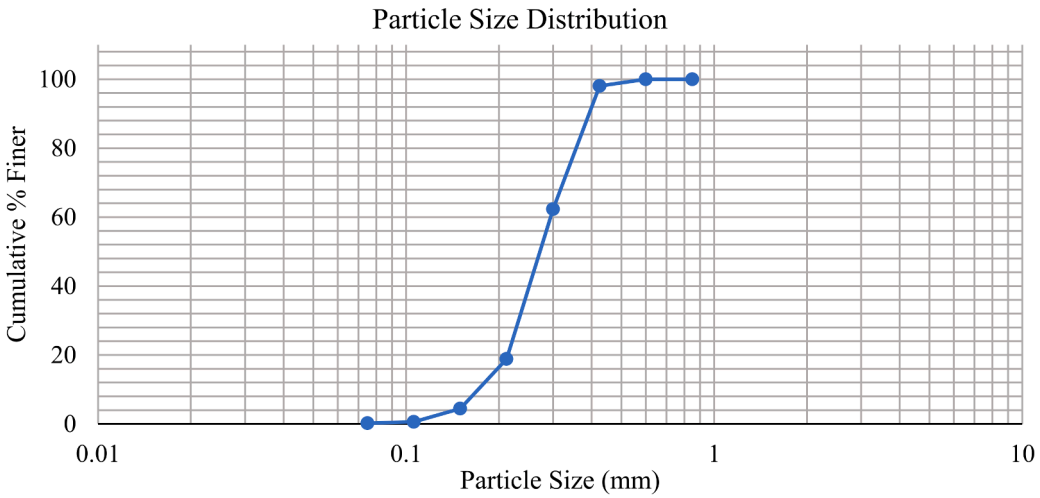

Fig. 1. Particle size distribution of Silica Sand.

2.4. Artificial lightweight fine aggregate (ALWFA)

High-strength functional ALWFA was created through a process involving the embedding of epoxy (mixture of epoxy resin and crosslinker; CM–ER–Thin, R&B Co. Ltd., Daejoen, South Korea) into the internal pores (ranging from approximately 0.3 to 300 μm) of the pristine ALWFA (Produced by mixing and firing coal ash and dredged soil, size ~1–5 mm, porosity~ 44 %, NDlite-LWA, Korea South-East Power Co., Ltd., Jinju-si, South Korea, refer to Korean standard F 2534) while also applying a coating to the external surface [29]. When hyper-crosslinked polymer (HCP) adheres to the internal pores of Lightweight Aggregate (LWA) particles, it strengthens the LWA through physical and chemical bonds with the porous surface, while preserving its lightweight properties. This study [29] proposed a method to enhance the functionality of LWAs by incorporating HCP for the adsorption and decomposition of air pollutants such as SO_x and NO_x, achieved by uniformly blending HCP with TiO_2. As HCP constitutes a permanent microporous polymer material, it forms a network of polymer chains through chemical reactions between monomers and crosslinkers. Epoxy resin, a typical HCP, was utilized to facilitate crosslinking and polymerization under mild reaction conditions. The resin, a high-viscosity substance convertible to polymers through crosslinking or polymerization, is mixed with a crosslinker (or hardener) and solidifies for application. Through the chemical bonding of epoxide groups to the inner surface pores of LWAs during crosslinking and polymerization, the LWA's strength is bolstered by additional physical and chemical bonds with the epoxy, while its lightweight characteristics remain intact.

The pristine ALWFA had a density of 1.4 g/cm^3 and a water absorption rate of 14.1 %. To eliminate surface pollutants, such as dust, the raw ALWFA underwent a washing procedure with running water and was subsequently air-dried for 15 h. An epoxy solution was prepared by mixing epoxy with isopropyl alcohol (IPA, DAEJUNG, Siheung-si, South Korea) and a fixed crosslinker at a concentration of 25 % by weight of epoxy resins. This epoxy solution was then combined with TiO_2 nanoparticles (sized approximately 300 nm, with a density of about 4.26 g/mL at (25 °C) rutile structure, ReagentPlus®, Sigma–Aldrich, St. Louis, MI, USA) at a mass ratio of 10:1. The mixture was sonicated to create an epoxy-TiO_2 composite solution (for detailed coating process, refer to Ref. [29]). The resulting epoxy-TiO_2 composite solution was introduced into the ALWFA under normal pressure coating conditions. In this process, ALWFAs were immersed in the epoxy-TiO_2 composite solution for 60 min at 20 °C under standard atmospheric pressure (1 atm). Afterward, the ALWFAs were taken out of the solution and left to air-dry for 8 h. Microscopic analysis was performed for ALWFA particles as shown in Fig. 2. From a visual examination of scanning electron microscopy (SEM) images in this figure, aggregate particles with a coating of epoxy–TiO_2 can be observed.

2.5. Mix proportion

In this study, the process followed several stages. First, dry components consisting of OPC, SF, SPW, SS, and ALWFA were blended for 5 min. Following this, a solution containing water and SP was added and mixed for an additional 5 min. The resulting mixture was then molded into samples: cubic shapes with dimensions 50 mm × 50 mm × 50 mm for conducting compressive strength tests and cylindrical forms measuring 200 mm × 100 mm for indirect tensile strength tests. These samples were allowed to cure at a controlled temperature of 25 ± 3 °C for a duration of 24 h. In this research, curing was carried out through two distinct approaches. After the initial 24-h curing phase, the samples were subjected to either 1) high-temperature curing at 90 °C and 95 % humidity for 2 days, followed by subsequent curing in standard room air conditions at 25 ± 3 °C, or 2) high-temperature curing at 90 °C and 95 % humidity for 2 days, followed by immersion in 25 °C water. These two methods were chosen to determine the most effective curing procedure [39].

Table 2 offers a comprehensive dataset concerning the mix development of the current work. According to this table, The Control Mix serves as the baseline, with standard quantities of OPC, SF, SPW, SS, and SP. No ALWFA is included. This mix provides a benchmark for comparing the effects of variations in ALWFA content in the subsequent mixes. LAC1 mixture features a reduced water, OPC, SF, and SPW content and includes ALWFA (25 %) as a lightweight aggregate and replacement for SS (75 %). LAC2 mixture maintains the reduced water, OPC, SF, and SPW content and includes a higher proportion of ALWFA (50 %) while decreasing SS (50 %) content. LAC3 mixture continues the trend of reduced water, OPC, SF, and SPW content and incorporates a significant amount of ALWFA (75 %) while further decreasing SS (25 %). LAC4 mixture eliminates SS entirely and incorporates a substantial amount of ALWFA (100 %), focusing on creating a lightweight concrete mix. By removing SS and increasing ALWFA, this mix ex-

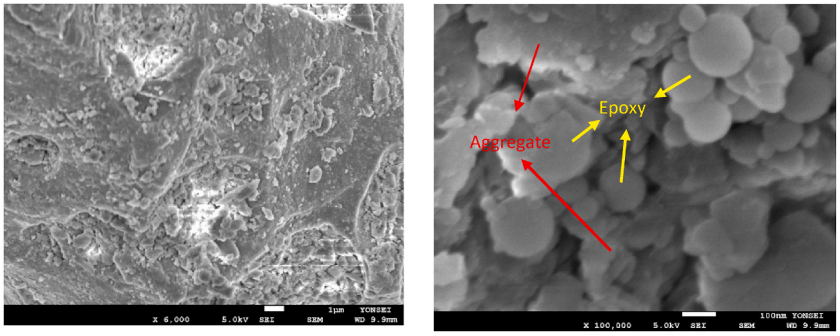

Fig. 2. Fabrication of an epoxy–TiO_2– embedded ALWFA.

Table 2
Mix design development.

Label	Water (kg/m^3)	Binder (kg/m^3)			Aggregate (kg/m^3)				SP (kg/m^3)
		OPC	SF	SPW (kg/m^3)	SS		ALWFA		
					%	kg	%	kg	
Control	208	832	208	208	100	915	0	0	9.6
LAC1	178.5	714	178.5	178.5	75	686	25	186	8.2
LAC2	178.5	714	178.5	178.5	50	458	50	372	8.2
LAC3	178.5	714	178.5	178.5	25	228	75	557	8.2
LAC4	178.5	714	178.5	178.5	0	0	100	743	8.2

plores the potential of achieving lightweight yet structurally viable concrete, offering advantages in specific construction scenarios where reduced weight is critical.

The study began by establishing the primary research objectives through a comprehensive review of existing literature. Subsequently, essential materials were procured and subjected to thorough evaluation of their chemical and physical properties. Following this, a suitable mix design was formulated based on prior research findings, guiding the casting of samples. These samples were then subjected to an initial curing phase at high temperature (90 °C) and 95 % humidity for 48 h. Subsequent investigations involved the implementation of two distinct curing conditions, namely air curing and water curing, aimed at assessing their respective impacts on the concrete's hardened properties. Finally, the study encompassed the evaluation of mechanical properties (including compressive and indirect tensile strength), microstructure analysis using SEM, and assessment of mineralogical composition through XRD analysis, effectively addressing the research objectives.

3. Experimental methods

3.1. Fresh properties - flow test

The flow table test serves as a technique employed to assess the workability and consistency of concrete. Its purpose is to gauge the concrete mix's ability to flow and self-compact under its own weight without the aid of mechanical vibration. This test is crucial for ensuring that the concrete can uniformly fill the formwork without experiencing segregation or excessive bleeding. By providing a quantitative measurement of concrete's flow properties, the flow table test offers a numerical value, unlike the qualitative assessment provided by the slump test. This numerical representation, obtained through the measured diameter of the concrete spread on the flow table, allows for easy comparison and monitoring of the concrete mix's flow characteristics over time. Therefore, in this work, the flow test was conducted to analyze the fresh performance of the LAC mixtures.

3.2. Mechanical performance

The concrete compressive strength test is a fundamental and vital assessment conducted to ensure concrete quality. It determines a concrete specimen's capacity to resist axial loads or forces applied along its axis without significant deformation. This strength measurement is pivotal in evaluating concrete's structural integrity and durability. In this research, batches of LAC were examined by casting and curing three cube specimens (50 × 50*50 mm) for each batch at three different ages of curing including 3, 7, and 28 days. A total of 90 cube specimens (18 samples per batch) were prepared for the compressive strength test. The compressive strength of LAC was tested at a loading rate of 0.5 MPa/s using cube specimens cured for 3, 7, and 28 days under two distinct curing methods. To analyze the mechanical performance of the samples, a digital motorized compression testing machine (Shingan SGB-201-1D) was employed. The assessment of compressive and indirect tensile strengths was conducted in compliance with the American standard ASTM c39/c39 m [40] and ASTM C496/C496 M [41], respectively.

The indirect split tensile strength of concrete is a critical characteristic that impacts the longevity, ability to resist cracks, and overall effectiveness of concrete structures. To assess tensile strength, this study involved casting and curing three cylindrical specimens (200 × 100 mm) for each concrete mixture. A total of 45 cylindrical samples (9 samples per batch) were prepared for the indirect tensile strength test. The curing procedure for the tensile test replicated the initial curing process applied in the compressive strength test (at three different ages of curing including 3, 7, and 28 days in the open air). Once demolded, the specimens were placed in an oven at a high temperature (90 °C) with 95 % humidity for 48 h and then left at room temperature in the open air until the testing day.

3.3. SEM analysis

The combination of Scanning Electron Microscopy (SEM) and energy-dispersive X-ray spectroscopy (EDS) offers powerful analytical tools for identifying distinct phases and chemical elements within concrete. This information is pivotal for comprehending the composition of concrete materials and their interactions, influencing the concrete's properties and longevity [42]. In this study, SEM with EDS was employed to examine the microstructure of concrete mixtures under both 3-day and 28-day curing conditions. Concrete powders were obtained following the completion of the compressive strength test. The SEM and EDS analyses were conducted using the Field Emission Scanning Electron Microscope (FE-SEM) 7800F-Prime (Fig. 3) machine as part of this research effort.

Fig. 3. FE-SEM 7800F-Prime machine.

3.4. XRD characterization

Understanding the mineralogical composition offers valuable insights into how concrete behaves in different situations, including issues like shrinkage, cracking, and long-term strength development. X-ray Diffraction (XRD) stands as a robust analytical method used to ascertain the chemical composition and crystallographic structure of various materials, concrete included. In concrete analysis, XRD plays a vital role in identifying the mineral composition of the crystalline phases within the concrete [43]. In this research, the crystallographic structure of LAC mixtures was analyzed using a Rigaku XRD (Ultima IV) machine with parameters including a copper (Cu) X-ray source, θ/2θ geometry, a scanning range of 5–80° 2θ, a step size of 0.02°, and a scanning speed of 2°/min (Fig. 4).

4. Results and discussion

4.1. Fresh properties

The results of the flow test, as illustrated in Table 3, reveal a noteworthy trend. It is evident that substituting ALWFA for fine aggregate has a significant adverse impact on the flow ability of the LAC mixtures. Specifically, the flowability values for the control, LAC1, LAC2, LAC3, and LAC4 mixes were 745 mm, 720 mm, 680 mm, 610 mm, and 475 mm, respectively. This decline in flowability correlates with the increase in ALWFA content.

This decrease in workability can be attributed to the presence of irregularly shaped ALWFA particles with sharp edges, which elevate internal friction within the concrete matrix. The heightened internal friction is the primary factor contributing to the reduction

Fig. 4. XRD (Ultima IV) machine.

Table 3
Flowability results.

Batch Num	Flowability (mm)
Control	745
LAC 1	720
LAC 2	680
LAC 3	610
LAC 4	475

in workability [44]. Conversely, when silica sand with spherical and regular particles is used as the fine aggregate, it results in reduced internal friction within the concrete matrix [45,46]. This reduction enhances the flowability, particularly in the control mix where 100 % silica sand was used as the fine aggregate, and a flowability of 745 mm was achieved. In addition to that, ALWFA is lightweight, which means it has a lower density than natural aggregates. The lower density can lead to poor particle packing and increased void content in the concrete mixture, reducing its flowability [47].

4.2. Compressive strength

The compressive strength results under air curing conditions are presented in Fig. 5. At the 3-day mark of normal curing, the compressive strength values for the control, LAC1, LAC2, LAC3, and LAC4 mixes were 164 MPa, 148 MPa, 140 MPa, 119 MPa, and 108 MPa, respectively. Notably, an increase in ALWFA content led to a decrease in compressive strength after the initial 3-day period of air curing. Upon reaching the 7-day point with the air curing method, the compressive strength values for the same mixes were 165 MPa, 160 MPa, 141 MPa, 130 MPa, and 125 MPa, respectively. Comparing these results to the 3-day data, it becomes evident that all samples experienced an increase in compressive strength. This enhancement can be attributed to the ongoing hydration process and the formation of calcium silicate hydrate gel (CSH gel) within the concrete matrix, which contributes to the development of strength over time [44,48,49].

The data from Fig. 5 Reveals the compressive strength values for the same mixtures at the 28-day mark of the normal curing period: 170 MPa for the control mix, 158 MPa for LAC1, 137 MPa for LAC2, 122 MPa for LAC3, and 114 MPa for LAC4, respectively. Upon analyzing these results, it becomes evident that, except for the control mix, there is a decline in the compressive strength of all other samples at 28 days compared to the results at 7 days of curing. The reduction in compressive strength observed at 28 days compared to 7 days for the UHPLC samples containing ALWFA can be attributed to several interrelated factors. ALWFA particles are inherently more porous than traditional SS, and during the curing process, they tend to lose internal moisture more rapidly. This moisture loss leads to the shrinkage of ALWFA particles, creating internal stresses within the concrete matrix. The shrinkage of the aggregate can cause micro-cracks at the interfacial transition zone between the ALWFA and the cement paste, weakening the overall structure. Additionally, the high porosity of ALWFA results in more void spaces within the aggregate. As water evaporates from these voids over time, the effective bonding area between the cementitious matrix and the aggregate decreases, contributing to the reduction in compressive strength.

During the initial curing period, the presence of water facilitates the hydration process, leading to strength development. However, as curing progresses, the internal moisture within the porous ALWFA particles continues to evaporate, causing differential drying and shrinkage within the concrete. This redistribution of moisture induces internal stresses and micro-cracking, further reducing compressive strength. In conventional concrete, prolonged water curing generally improves compressive strength due to continued hydration. However, in UHPLC containing ALWFA, the benefit of extended water curing may be offset by the internal drying and shrinkage stresses induced by the ALWFA. This unique behavior results in a decrease in compressive strength at 28 days compared to 7 days. The initial hydration of UHPLC with ALWFA may be more rapid due to the high reactivity of supplementary cementitious materials like fly ash, silica fume, and silica powder. However, as the hydration process progresses, the internal shrinkage and drying of ALWFA can disrupt the continued hydration of these materials, leading to a plateau or even a decrease in strength gain. Moreover, the ongoing shrinkage of ALWFA can lead to the formation and propagation of micro-cracks within the concrete matrix. These micro-cracks compromise the integrity of the concrete, resulting in a reduction in compressive strength over time. The presence of these micro-cracks is likely more pronounced at 28 days, accounting for the observed decrease in strength. In summary, the reduction in compressive strength of UHPLC containing ALWA at 28 days compared to 7 days is primarily due to the shrinkage and high porosity of the ALWA, which induces internal stresses and micro-cracking, along with the redistribution of internal moisture and the consequent disruption of the hydration process. These factors collectively undermine the structural integrity of the concrete over time, leading to a decrease in compressive strength at the later curing stage. Conversely, the control mix displayed an increase in compressive strength

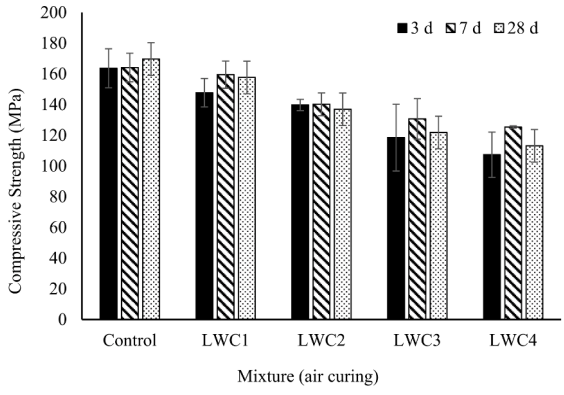

Fig. 5. Compressive strength results with air curing condition.

at the 28-day mark of normal curing, indicating the continued hydration process within the concrete matrix. This observation underscores the significance of the hydration process in enhancing the strength properties of the control mix over an extended curing period.

The diminished compressive strength of concrete containing ALWFA, as compared to normal concrete, can be attributed to various factors. Firstly, ALWFA particles generally possess higher porosity in contrast to natural aggregates. These pores within the aggregates create weak spots in the concrete, diminishing its overall compressive strength [50]. These pores serve as stress concentrators, rendering the concrete more vulnerable to failure under compression. Secondly, ALWFA particles often exhibit lower intrinsic strength when compared to dense natural aggregates. This reduced strength directly impacts the overall compressive strength of the concrete when these weaker aggregates are integrated into the mix. Thirdly, the cohesion between ALWFA particles and the surrounding matrix might be weaker due to their porous and lightweight nature. This decreased cohesion can result in lower compressive strength, as the aggregates may not effectively transfer compressive stresses within the concrete. Lastly, the interface between ALWFA particles and the cement paste might be weaker than in normal concrete due to the porous nature of ALWFA. Weak bonding between aggregates and the paste reduces the compressive strength of the concrete. These combined factors contribute to the inferior compressive strength observed in concrete containing artificial lightweight aggregates.

The compressive strength data under water curing conditions is displayed in Fig. 6. At the 3-day mark of normal curing, the compressive strength values for the control, LAC1, LAC2, LAC3, and LAC4 mixes were 157 MPa, 148 MPa, 126 MPa, 111 MPa, and 107 MPa, respectively. These results indicate a decrease in compressive strength corresponding to the increase in ALWFA content, mirroring the findings from the normal curing condition. It is noteworthy that the compressive strength values at 3 days of water curing were slightly lower than those observed under air curing conditions. This disparity can be attributed to the slower development of the hydration process in water curing conditions in comparison to the normal curing method. After 7 days of water curing, there was a marginal uptick in the compressive strength of all mixtures. Specifically, the compressive strength values for the same mixes were 158 MPa, 149 MPa, 133 MPa, 125 MPa, and 108 MPa, respectively. This increase can be attributed to the ongoing development of the hydration process within the concrete matrix during the early stages. The continued chemical reactions and bonding mechanisms between cement particles and water molecules are the primary factors contributing to the rise in compressive strength observed at the 7-day mark of water curing.

Upon reaching the 28-day mark in the water curing conditions, the compressive strength values for the same mixes were 140 MPa, 135 MPa, 123 MPa, 109 MPa, and 100 MPa, respectively. Analyzing these data reveals a gradual reduction in the compressive strength of all mixes compared to the results observed at 7 days of water curing. Similar to the normal curing condition, shrinkage emerges as the primary factor contributing to the diminished compressive strength at the 28-day mark of water curing. Although water curing maintains a consistent moisture content in the concrete, it does not entirely eliminate the possibility of shrinkage. Concrete can still experience drying shrinkage as it loses moisture, leading to a decrease in volume [51]. This shrinkage, albeit to a lesser extent compared to concrete cured in dry conditions, can result in cracking and impact the overall dimensions and structural integrity of the concrete.

In summary, the higher compressive strength of concrete samples in normal (air) curing conditions, as compared to water curing conditions, can be attributed to several factors. Firstly, concrete samples in air curing conditions are exposed to air, facilitating the gradual evaporation of excess water within the concrete. This drying process leads to a more compact and dense structure, enhancing the compressive strength of the concrete. Secondly, exposure to air allows for the continuous progression of chemical reactions within the concrete matrix. These reactions, especially the hydration of cement particles, persist over time, resulting in the formation of additional binding materials such as CSH gel. This ongoing chemical activity significantly contributes to the development of higher compressive strength in air-cured concrete. Thirdly, although water curing maintains a consistent moisture environment, the curing rate in water is generally slower compared to air curing. Concrete gains strength through the hydration process, which relies on the presence of water. In a water-curing environment, the availability of water may be limited due to the slow diffusion of water into the inte-

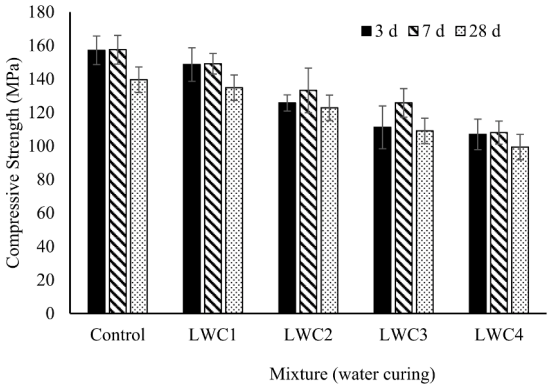

Fig. 6. Compressive strength results with water curing condition.

rior of the concrete. This limitation results in a slower strength development when compared to concrete exposed to air. Furthermore, water curing can lead to the leaching of calcium hydroxide and other soluble compounds from the concrete, potentially weakening the structure and reducing the compressive strength of the concrete over time. Additionally, air-cured concrete is often exposed to ambient temperatures, which might be higher than the curing water temperature. Elevated temperatures can accelerate the hydration reactions, leading to faster strength gain in air-cured samples. Finally, the microstructure of air-cured concrete differs from that of water-cured concrete. Air-cured concrete tends to possess a more refined and well-developed microstructure, a characteristic that significantly contributes to its higher compressive strength. It is important to highlight that incorporating silica fume into the concrete mix as a cementitious material can boost pozzolanic activity and create secondary CSH gel during prolonged curing periods, extending beyond 90 days. This enhancement results in a rise in compressive strength. This development underscores the opportunity to adjust the mix design, potentially improving the concrete's long-term compressive properties.

4.3. Indirect tensile strength

Fig. 7 illustrates the results of the indirect spilite tensile strength test. At the 3-day mark of normal (air) curing, the tensile strength values for the control, LAC1, LAC2, LAC3, and LAC4 mixes were 8.20 MPa, 6.81 MPa, 4.84 MPa, 3.44 MPa, and 4.28 MPa, respectively. Notably, an increase in ALWFA content led to a decrease in tensile strength, except for the LAC4 mixture. Concrete mixtures incorporating ALWFA generally exhibit lower tensile strength compared to standard concrete due to several factors. ALWFA particles typically have higher porosity than natural aggregates, creating weak points within the concrete [46]. These pores act as stress concentrators, making the concrete more vulnerable to cracking under tensile loads. Additionally, the interface between ALWFA particles and the cement paste tends to be weaker than in normal concrete because of the porous nature of ALWFA particles. This weak bonding reduces the overall tensile strength of the concrete. This trend is consistent during the 7-day curing period, where the indirect tensile strength for the same mixes was 6.48 MPa, 5.77 MPa, 4.54 MPa, 4.18 MPa, and 4.13 MPa, respectively. The results reaffirm the impact of increased ALWFA content on decreasing the tensile strength of the concrete mixtures.

As mentioned earlier, several factors contribute to the lower tensile strength in these mixtures: Firstly, ALWFA particles generally possess higher porosity compared to natural aggregates. This increased porosity creates internal voids and weak points within the concrete matrix. Under tensile loads, these pores act as stress concentrators, which facilitate crack initiation and propagation, thereby reducing the overall tensile strength. Secondly, the interface between the ALWFA particles and the cement paste is typically weaker than that found in concrete with natural aggregates. The porous nature of ALWFA leads to a less robust bond at the interfacial transition zone (ITZ). This weaker bonding at the ITZ contributes significantly to the reduced tensile strength, as the concrete becomes more susceptible to cracking along these weaker interfaces. Thirdly, the inclusion of ALWFA introduces greater heterogeneity in the concrete mix. This heterogeneity can lead to uneven stress distribution under tensile loading, further exacerbating the material's vulnerability to cracking and reducing its tensile strength. Finally, while our study did not specifically measure shrinkage, it is known that high cement content and the use of lightweight aggregates like ALWFA can contribute to higher shrinkage rates. Increased shrinkage can lead to micro-cracking, which negatively affects tensile strength.

From Fig. 7, the indirect tensile strength of the same mixtures at the 28-day maturity mark can be observed: 7.28 MPa for the control mix, 6.67 MPa for LAC1, 5.44 MPa for LAC2, 4.19 MPa for LAC3, and 3.79 MPa for LAC4. These results align with the compressive strength findings at the 28-day normal curing period. Consequently, the same factors contributing to shrinkage during the later stages of the curing period could be the primary cause for the reduction in indirect tensile strength at the 28-day curing point. It is worth noting that the addition of silica fume as a cementitious material in the concrete matrix can enhance pozzolanic activity over extended curing periods (beyond 90 days), leading to an increase in tensile strength. This improvement highlights the potential for modifying the mix design to positively impact the concrete's tensile properties in the long term.

Regarding the low splitting tensile strength relative to the compressive strength observed in this study, it would be beneficial to compare our results with those from previous studies on high-performance lightweight concrete. Referring to the existing literature can provide a more comprehensive understanding and context for our findings. In this respect, Arioglu et al. [52] indicated that light-

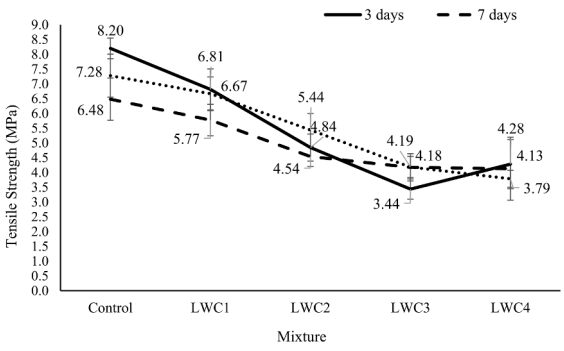

Fig. 7. Indirect tensile strength results with air curing condition.

weight aggregates, particularly those with high porosity, can significantly impact the tensile strength due to the creation of weak points within the concrete matrix. Their study has shown that the addition of lightweight aggregates led to a reduction in tensile strength compared to the compressive strength, primarily because the porous nature of these aggregates weakens the bond with the cement paste and acts as stress concentrators under tensile loads. In addition to that in a study on high-strength lightweight concrete incorporating graphene oxide [53], the results showed that although the mechanical properties improved, the ratio of splitting tensile strength to compressive strength remained lower than that typically found in conventional concrete, reflecting the inherent challenges posed by lightweight aggregates.

4.4. SEM investigation

The findings from Scanning Electron Microscopy (SEM) and energy dispersive X-ray spectroscopy (EDS) conducted under standard curing conditions for 3 days are depicted in Fig. 8. All SEM images had a size of 1 μm, with magnifications ranging from x5000 to x20000. Furthermore, SEM analysis was conducted on particles collected from the cross-sections of the samples. SEM analysis indicated that an increase in ALWFA content as a substitute for fine aggregate leads to a rise in the quantity of voids. This could be attributed to the porous nature of ALWFA particles, potentially being a significant factor in the decline of compressive strength with escalating ALWFA content as a fine aggregate replacement [54]. The circled regions in the micrographs represent the voids, while the remainder comprises calcium silicate hydrate (C–S–H) gel, calcium hydroxide crystals (CH), ettringite (E), and aggregate.

Furthermore, the energy dispersive X-ray spectroscopy (EDS) map sum spectrum reveals that O, Si, and Ca are the primary elements in the structure of all mixtures with varying proportions. These results align with the XRD findings, where quartz (SiO_2) and Alite (Tricalcium silicate: Ca_3SiO_5) emerge as the principal crystalline phases [55]. It should be noted that the EDS was conducted on the entire SEM image rather than marking specific zones point by point. This approach was selected to obtain a comprehensive and unbiased analysis of the elemental composition across the entire sample surface, ensuring that the data reflects the overall distribu-

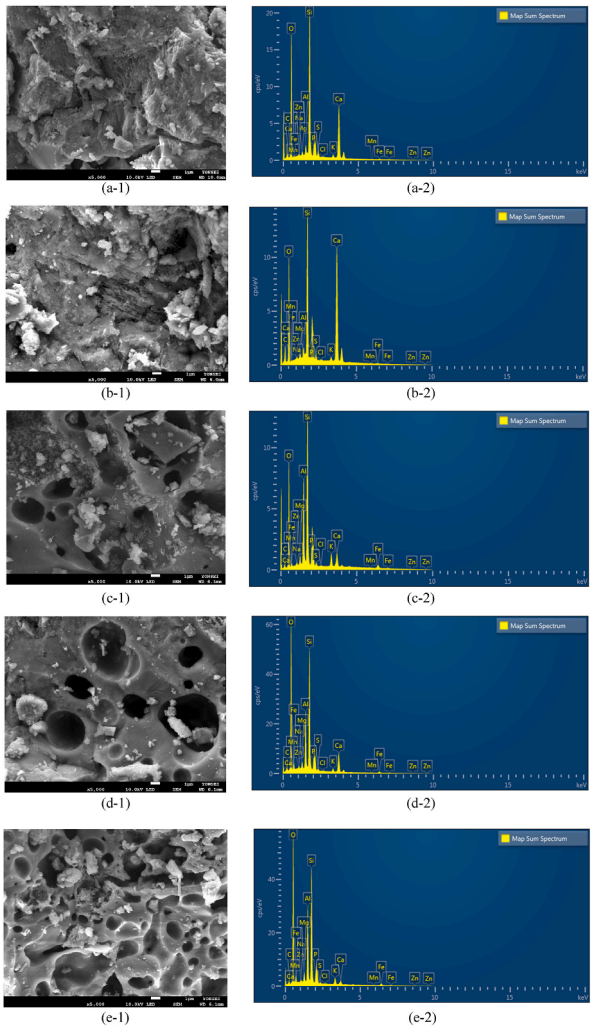

Fig. 8. SEM images and EDS maps after 3 days of curing period for samples a) control, b) LAC1, c) LAC2, d) LAC3, and e) LAC4.

tion of elements rather than localized areas. In summary, the SEM results after a 3-day curing period demonstrate a noticeable structural difference in LAC mixtures due to the presence of ALWFA particles. Conversely, the EDS results indicate no significant disparity in the composition of all mixtures.

Comparable outcomes were noted in both SEM images and EDS maps following a 28-day curing duration (Fig. 9). This indicates that, under standard curing conditions for 28 days, there was an increase in the number and size of voids due to the higher proportion of ALWFA replacing fine aggregate. The incorporation of SF as a partial substitute for OPC enhances the potential for secondary CSH gel formation after extended curing periods (beyond 90 days). Consequently, beyond 28 days, the generation of additional CSH gel becomes imperceptible. Conversely, owing to the significant void content in LAC mixtures, the evaporation of internal water within ALWFA particles due to shrinkage resulted in a reduction in compressive strength compared to the results at 7 days.

The EDS map spectrum results for all mixtures after a 28-day curing period exhibited a nearly identical composition to their 3-day counterparts. This consistency may be attributed to the lack of substantial changes in the structure and composition of all mixtures post the specified curing period. In all samples, O, Si, and Ca remained the primary elements, consistent with the EDS map spectrum results. These findings align with the results of XRD analysis, where quartz and alite persist as the principal crystalline phases in the structure of all mixtures.

4.5. XRD analysis

The X-ray Diffraction (XRD) patterns of concrete mixtures incorporating varying proportions of Artificial Lightweight Fine Aggregate (ALWFA) at 3 days and 28 days of the curing period are illustrated in Figs. 10 and 11. Predominant crystalline phases identified in most samples after both 3 days and 28 days of curing include Quartz (SiO_2), Alite (Tricalcium silicate: Ca_3SiO_5), Calcite ($CaCO_3$), and Andradite ($Ca_3Fe_2(SiO_4)_3$). The presence of SF as a partial replacement for cement in concrete can influence the XRD pattern, including the 2θ values of diffraction peaks. However, these changes are usually subtle, especially for the primary crystalline phases like

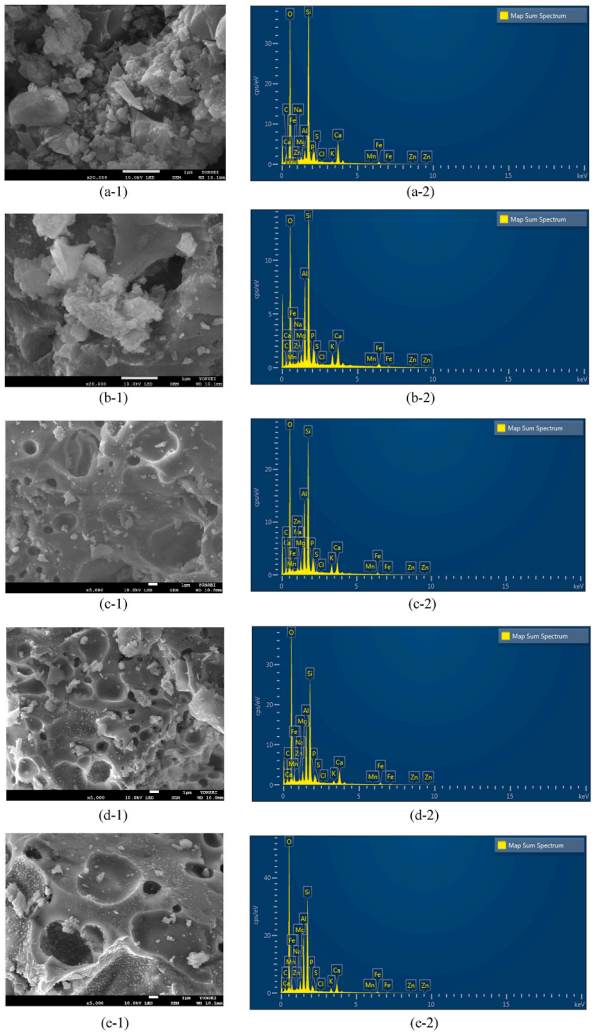

Fig. 9. SEM images and EDS maps after 28 days of curing period for samples a) control, b) LAC1, c) LAC2, d) LAC3, and e) LAC4.

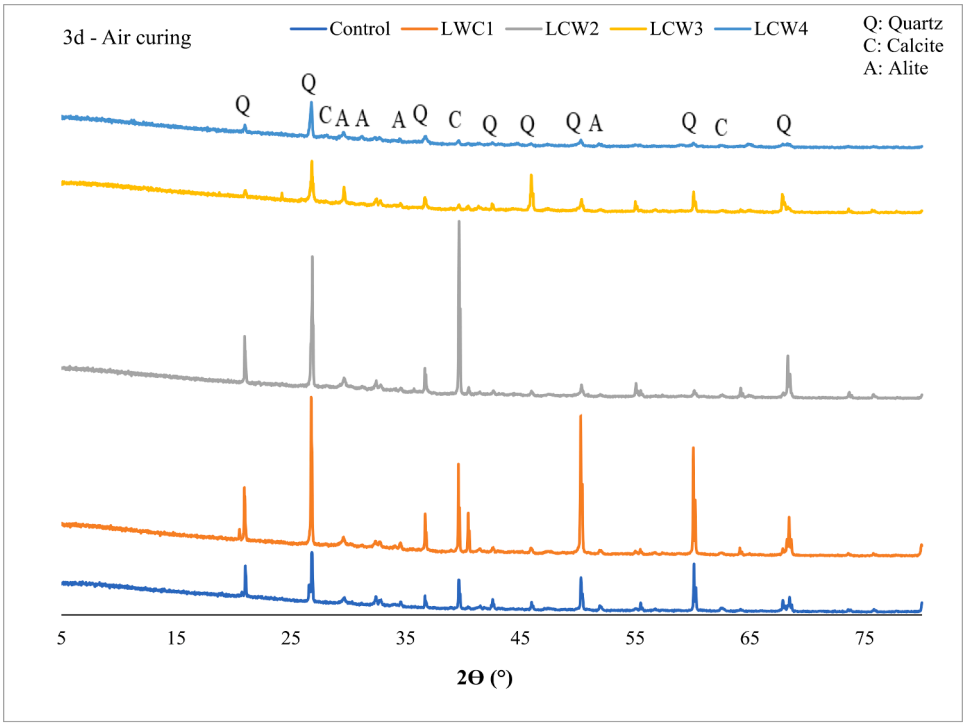

(a) 3d – Air curing

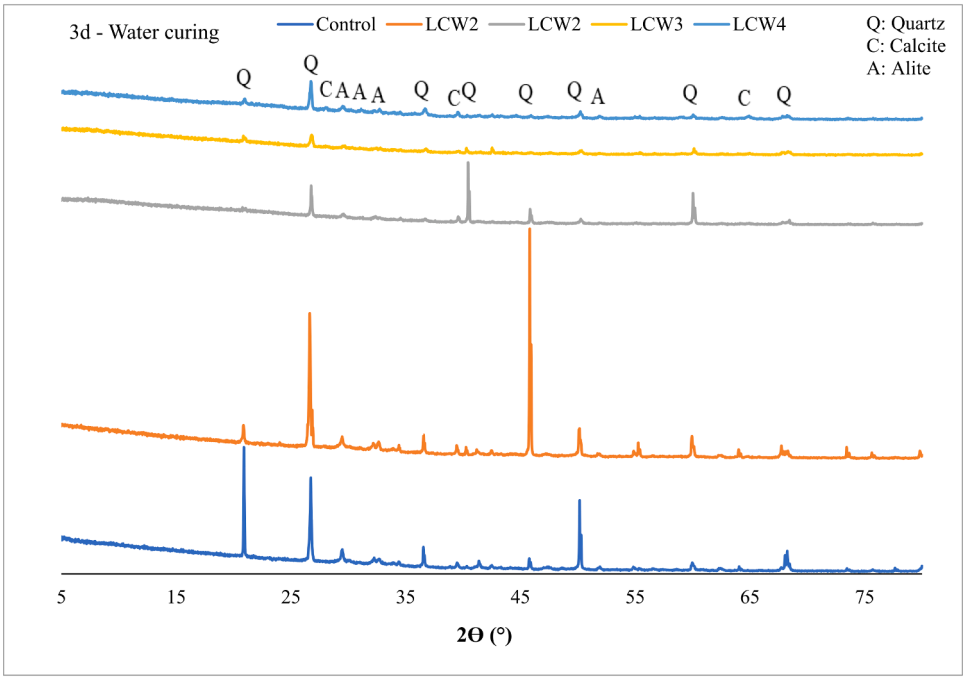

(b) 3d – Water curing

Fig. 10. XRD Analysis of a) 3d – Air curing, and b) 3d – Water curing condition.

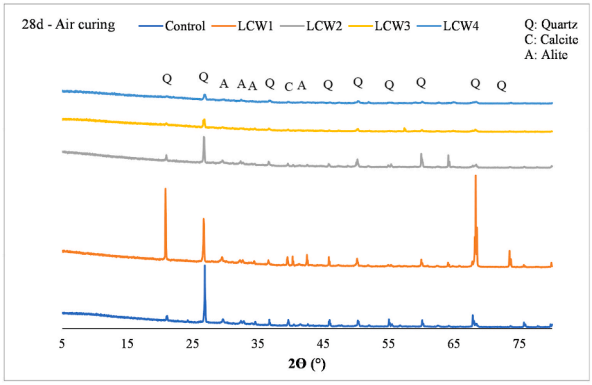

(a) 28d – Air curing

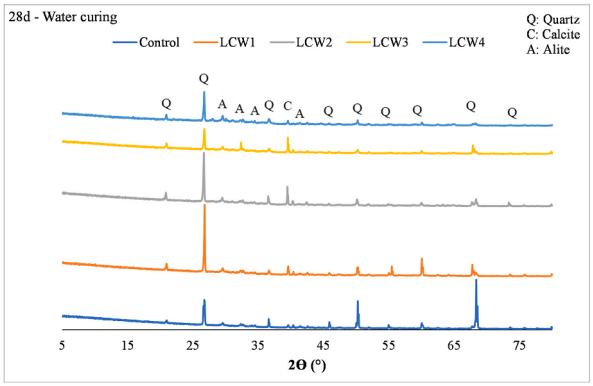

(b) 28d – Water curing

Fig. 11. XRD Analysis of a) 28d – Air curing, and b) 28d – Water curing condition.

quartz, calcite [54]. Notably, the presence of Alite (which contributes significantly to the early strength development in concrete) in the control mix during 3 days of air curing was higher compared to water curing, as depicted in Fig. 10a. Conversely, the occurrence of quartz was higher in 3 days water-cured samples than in those air-cured. This trend persisted in the LAC1 mixture, possibly contributing to the increased compressive strength of air-cured samples in comparison to their water-cured counterparts.

In contrast, for LAC2 and LAC3 samples, the intensity of quartz in 3 days air curing exceeded that in 3 days water curing, likely due to the elevated ALWFA content in these mixes (Fig. 10a and b). The observed disparities in compressive strength between air and water-cured samples may be influenced by factors related to curing conditions, rather than changes in quartz content. In general, the combination of silica-rich materials, favorable temperature and pressure conditions, chemical reactions, and aggregate characteristics likely contributes to the formation of quartz observed in the XRD pattern of this study. However, it should be noted that while the mentioned factors may contribute to the presence of quartz in the XRD pattern, it's essential to consider the specific conditions and processes involved. Quartz typically forms through natural geological processes over long periods, primarily involving the crystallization of silicon dioxide under specific temperature and pressure conditions. However, in the context of the study, the combination of silica-rich materials, temperature, pressure, chemical reactions, and aggregate characteristics might facilitate the crystallization or transformation of existing silica compounds into quartz-like structures under certain conditions. This explanation highlights the complexity of mineral formation processes and acknowledges the need for further investigation and analysis to fully understand the mechanisms involved. However, the XRD patterns of the LAC4 mixture, where 100 % ALWFA replaced the fine aggregate, exhibited comparable trends in both water and air curing conditions. This consistency sheds light on the similar compressive strength observed for the LAC4 mixture after a 3-day curing period under both water and air curing conditions (Fig. 10a and b). These findings emphasize the intricate interplay between ALWFA content, curing methods, and the resultant crystalline phases, significantly impacting the concrete's compressive

strength.

The XRD analysis results at the 28-day mark under both curing conditions (as depicted in Fig. 11) exhibited notable differences compared to the 3-day curing period. Across all mixtures, the presence of quartz during the 28-day water curing conditions exceeded that in the 28-day air curing conditions. Conversely, the concentrations of alite and calcite in all mixtures were higher in the 28-day air curing conditions compared to the 28-day water curing conditions. This discrepancy elucidates the compressive strength results for these mixtures, where after 28 days of air curing, the compressive strength marginally surpassed that of the 28-day water curing. The heightened content of alite in the air curing conditions likely contributed to the increase in compressive strength through this curing method. It is worth noting that due to the exceptionally low permeability of Ultra-High-Performance Lightweight Concrete (UH-

PLC), water curing did not positively impact its performance. The hydration process following the initial high-temperature curing (within the first 48 h post-demolding) occurred at a faster rate under normal curing conditions compared to water curing conditions.

Moreover, it is crucial to acknowledge that after 28 days of both curing methods, no new crystalline phases emerged in any of the mixtures. This implies the absence of pozzolanic activity within the initial 28-day curing period. To induce pozzolanic activity, a prolonged curing period, exceeding 90 days, is required. Additionally, upon comparing Figs. 10 and 11, it is evident that the intensity of most phases slightly diminished after 28 days under both curing conditions compared to their 3-day intensity. This reduction in intensity could be attributed to the shrinkage process within the mixtures. This shrinkage process is responsible for the decrease in compressive strength observed in most mixtures after 28 days under both curing conditions in contrast to their 3-day compressive strength.

Based on the results obtained from the XRD analysis, it can be concluded that there is no notable alteration in the crystalline phases with the increase in ALWFA content as a substitute for fine aggregate. The primary phases observed in all samples, namely quartz, alite, and calcite, remained consistent. This consistency can be attributed to the higher binder content (Ordinary Portland Cement and Silica Fume) in comparison to the aggregate content. Additionally, the prevalence of quartz as the primary crystalline phase across all mixtures can be attributed to the incorporation of silica fume, silica sand, and silica powder in the concrete formulations. These findings underscore the stability of the main crystalline phases and highlight the influence of binder composition on the overall composition of the concrete samples. Upon comparing the results of SEM and XRD analyses, it becomes evident that the findings underscore the complex interplay among ALWFA content, curing methods, and resulting crystalline phases, all of which profoundly influence concrete's compressive strength. SEM analysis visually demonstrated void formation attributed to ALWFA particles, whereas XRD analysis elucidated the influence of curing conditions on crystalline phase presence, thereby impacting compressive strength outcomes.

5. Conclusion

In this investigation, ultra-high-performance lightweight concrete was manufactured by incorporating ALWFA as a partial or complete substitute for fine aggregate. The study assessed the fresh performance and mechanical properties of the lightweight concrete (LAC) mixtures through flow tests, as well as compressive and tensile strength tests, respectively. Microstructural changes in the LAC mixtures were analyzed using SEM images along with EDS maps. Additionally, the crystalline phase of the materials was examined through the application of the XRD method. Consequently, the current research yields the following outcomes.

1. The outcomes of the flow test indicate that as the proportion of ALWFA replacing fine aggregate increases, workability diminishes. The irregularly shaped ALWFA particles with sharp edges escalate internal friction, likely constituting the primary cause behind the decreased workability in LAC mixtures. Additionally, suboptimal particle packing and an augmented void content may contribute as additional factors leading to the reduced flowability of LAC mixtures.
2. The results of both compressive and tensile strength tests indicated a reduction in both parameters with an increasing proportion of ALWFA as a substitute for fine aggregate. Furthermore, the examination of various curing conditions revealed that the air curing method outperformed the water curing method. Consequently, the compressive strength results for the air curing condition were marginally higher than those for the water curing condition. This difference can be attributed to the exposure of concrete samples in air curing conditions to the air, facilitating the gradual evaporation of excess water within the concrete. This drying process contributes to a more compact and dense structure, ultimately enhancing the compressive strength of the concrete.
3. The SEM analysis revealed that elevating the ALWFA content as a replacement for fine aggregate resulted in an increase in both the number and dimensions of voids. This phenomenon can be ascribed to the porous characteristics of ALWFA particles, potentially playing a crucial role in the diminishing compressive strength observed as the ALWFA content rises as a substitute for fine aggregate. Additionally, the energy dispersive X-ray spectroscopy (EDS) map sum spectrum highlights that oxygen (O), silicon (Si), and calcium (Ca) are the predominant elements present in the structure of all mixtures, albeit in different proportions.
4. Drawing conclusions from the XRD analysis results, it can be asserted that there is no significant alteration in the crystalline phases as the ALWFA content increases as a replacement for fine aggregate. The primary phases identified in all samples, namely quartz, alite, and calcite, remained unchanged. This consistency can be attributed to the higher binder content (comprising Ordinary Portland Cement and Silica Fume) relative to the aggregate content. Moreover, the dominance of quartz as the principal crystalline phase in all mixtures is linked to the inclusion of silica fume, silica sand, and silica powder in the concrete formulations.

Based on the findings of this study, it is evident that ultra-high-performance lightweight concrete incorporating ALWFA as a substitute for fine aggregate can be manufactured with satisfactory mechanical performance. Subsequent research endeavors could delve into the long-term performance of lightweight concrete (LAC) mixtures, extending the investigation beyond a 90-day curing period. Additionally, future studies may explore the performance of LAC mixtures in challenging environments, assessing their resistance under conditions such as acid attack and sulfate attack, and elevated temperature condition. In addition, drying shrinkage of LAC mixtures should be investigated by future study to provide a more comprehensive understanding of the behavior of UHPLC with ALWA. Finally, it is suggested that future studies focus on comprehensive ASR testing to further understand the potential effects of ALWFA on concrete durability.

CRediT authorship contribution statement

Mahdi Rafieizonooz: Writing – review & editing, Writing – original draft, Methodology, Data curation, Conceptualization. **Jang-Ho Jay Kim:** Writing – review & editing, Supervision, Project administration, Funding acquisition. **Jin-su Kim:** Validation, Investigation, Data curation. **Jae-Bin Jo:** Methodology, Investigation, Data curation. **Elnaz Khankhaje:** Writing – review & editing, Methodology, Conceptualization.

Declaration of competing interest

The authors declare that they have no known competing financial interests or personal relationships that could have appeared to influence the work reported in this paper.

Data availability

Data will be made available on request.

Acknowledgment

This work is supported by the Korea Agency for Infrastructure Technology Advancement (KAIA) grant funded by the Ministry of Land, Infrastructure and Transport (Grant RS-2020-KA156177).

References

[1] Y. Zhang, Y. Hua, X. Zhu, Investigation of the durability of eco-friendly concrete material incorporating artificial lightweight fine aggregate and pozzolanic minerals under dual sulfate attack, J. Clean. Prod. 331 (2022) 130022, https://doi.org/10.1016/j.jclepro.2021.130022.
[2] L.P. Qian, B.T. Huang, L.Y. Xu, J.G. Dai, Concrete made with high-strength artificial geopolymer aggregates: mechanical properties and failure mechanisms, Construct. Build. Mater. 367 (2023) 130318, https://doi.org/10.1016/J.CONBUILDMAT.2023.130318.
[3] K.H. Yang, J.H. Mun, S. Kim, C.R. Im, Y.B. Jung, Seismic performance of precast lightweight aggregate concrete shear walls with supplementary V-ties, Eng. Struct. 297 (2023) 117000, https://doi.org/10.1016/J.ENGSTRUCT.2023.117000.
[4] S. İpek, O.A. Ayodele, K. Mermerdaş, Influence of artificial aggregate on mechanical properties, fracture parameters and bond strength of concretes, Construct. Build. Mater. 238 (2020) 117756, https://doi.org/10.1016/J.CONBUILDMAT.2019.117756.
[5] A. Terzić, L. Pezo, V. Mitić, Z. Radojević, Artificial fly ash based aggregates properties influence on lightweight concrete performances, Ceram. Int. 41 (2015) 2714–2726, https://doi.org/10.1016/J.CERAMINT.2014.10.086.
[6] M. Rafieizonooz, M.R. Salim, M.W. Hussin, J. Mirza, S.M. Yunus, E. Khankhaje, Workability, Compressive Strength & Leachability of Coal Ash Concrete, 2017, https://doi.org/10.3303/CET1756074.
[7] K.S. Vali, S. Bala Murugan, Performance of manufactured aggregate in the production of sustainable lightweight concrete, Mater. Today Proc. 60 (2022) 674–680, https://doi.org/10.1016/J.MATPR.2022.02.314.
[8] J. Lin, T.H. Tan, J.S. Yeo, Y. Goh, T.C. Ling, K.H. Mo, Municipal woody biomass waste ash-based cold-bonded artificial lightweight aggregate produced by one-part alkali-activation method, Construct. Build. Mater. 394 (2023) 131619, https://doi.org/10.1016/J.CONBUILDMAT.2023.131619.
[9] B. Wang, L. Yan, Q. Fu, B. Kasal, A comprehensive review on recycled aggregate and recycled aggregate concrete, Resour. Conserv. Recycl. 171 (2021) 105565, https://doi.org/10.1016/J.RESCONREC.2021.105565.
[10] I. Wichmann, D. Stephan, Mechanical and physical properties of concrete made of alkali-activated lightweight aggregates from construction demolition waste, Mater. Today Proc. (2023), https://doi.org/10.1016/J.MATPR.2023.05.533.
[11] A. Akhtar, A.K. Sarmah, Novel biochar-concrete composites: manufacturing, characterization and evaluation of the mechanical properties, Sci. Total Environ. 616–617 (2018) 408–416, https://doi.org/10.1016/J.SCITOTENV.2017.10.319.
[12] Y. Jiang, T.C. Ling, M. Shi, Strength enhancement of artificial aggregate prepared with waste concrete powder and its impact on concrete properties, J. Clean. Prod. 257 (2020) 120515, https://doi.org/10.1016/J.JCLEPRO.2020.120515.
[13] Z. Shen, H. Zhu, Z. Zhao, S. Pang, Z. Li, S. Yang, P. Cao, S. Lin, High-performance artificial aggregate prepared with recycled concrete powder and its impact on concrete properties, Construct. Build. Mater. 404 (2023) 133151, https://doi.org/10.1016/J.CONBUILDMAT.2023.133151.
[14] M. Rafieizonooz, E. Khankhaje, S. Rezania, Assessment of environmental and chemical properties of coal ashes including fly ash and bottom ash, and coal ash concrete, J. Build. Eng. 49 (2022) 104040, https://doi.org/10.1016/J.JOBE.2022.104040.
[15] M. Rafieizonooz, M.R. Salim, J. Mirza, M.W. HussinSalmiati, R. Khan, E. Khankhaje, Toxicity characteristics and durability of concrete containing coal ash as substitute for cement and river sand, Construct. Build. Mater. 143 (2017), https://doi.org/10.1016/j.conbuildmat.2017.03.151.
[16] M. Rafieizonooz, J. Mirza, M.R. Salim, M.W. Hussin, E. Khankhaje, Investigation of coal bottom ash and fly ash in concrete as replacement for sand and cement, Construct. Build. Mater. 116 (2016) 15–24, https://doi.org/10.1016/j.conbuildmat.2016.04.080.
[17] Q. Dong, G. Wang, X. Chen, J. Tan, X. Gu, Recycling of steel slag aggregate in portland cement concrete: an overview, J. Clean. Prod. 282 (2021) 124447, https://doi.org/10.1016/J.JCLEPRO.2020.124447.
[18] M. Xu, Y. Zhang, S. Yang, L. Mo, P. Liu, Effects of internal CO2 curing provided by biochar on the carbonation and properties of steel slag-based artificial lightweight aggregates (SALAs), Cem. Concr. Compos. 142 (2023) 105197, https://doi.org/10.1016/J.CEMCONCOMP.2023.105197.
[19] E. del Rey Castillo, N. Almesfer, O. Saggi, J.M. Ingham, Light-weight concrete with artificial aggregate manufactured from plastic waste, Construct. Build. Mater. 265 (2020) 120199, https://doi.org/10.1016/J.CONBUILDMAT.2020.120199.
[20] Y.W. Choi, D.J. Moon, Y.J. Kim, M. Lachemi, Characteristics of mortar and concrete containing fine aggregate manufactured from recycled waste polyethylene terephthalate bottles, Construct. Build. Mater. 23 (2009) 2829–2835, https://doi.org/10.1016/J.CONBUILDMAT.2009.02.036.
[21] S. Safinia, A. Alkalbani, Use of recycled plastic water bottles in concrete blocks, Procedia Eng. 164 (2016) 214–221, https://doi.org/10.1016/J.PROENG.2016.11.612.
[22] J. Ahn, J. Moon, J. Pae, H.K. Kim, Microplastics as lightweight aggregates for ultra-high performance concrete: mechanical properties and autoignition at elevated temperatures, Compos. Struct. 321 (2023) 117333, https://doi.org/10.1016/J.COMPSTRUCT.2023.117333.
[23] W. Dong, W. Li, Z. Tao, A comprehensive review on performance of cementitious and geopolymeric concretes with recycled waste glass as powder, sand or cullet, Resour. Conserv. Recycl. 172 (2021) 105664, https://doi.org/10.1016/J.RESCONREC.2021.105664.
[24] K. Kohno, T. Okamoto, Y. Isikawa, T. Sibata, H. Mori, Effects of artificial lightweight aggregate on autogenous shrinkage of concrete, Cement Concr. Res. 29 (1999) 611–614, https://doi.org/10.1016/S0008-8846(98)00202-6.
[25] Z. Li, W. Zhang, H. Jin, X. Fan, J. Liu, F. Xing, L. Tang, Research on the durability and Sustainability of an artificial lightweight aggregate concrete made from municipal solid waste incinerator bottom ash (MSWIBA), Construct. Build. Mater. 365 (2023) 129993, https://doi.org/10.1016/J.CONBUILDMAT.2022.129993.
[26] E. Güneyisi, M. Gesoglu, T. Özturan, S. Ipek, Fracture behavior and mechanical properties of concrete with artificial lightweight aggregate and steel fiber, Construct. Build. Mater. 84 (2015) 156–168, https://doi.org/10.1016/J.CONBUILDMAT.2015.03.054.
[27] J. Liu, Z. Li, W. Zhang, H. Jin, F. Xing, L. Tang, The impact of cold-bonded artificial lightweight aggregates produced by municipal solid waste incineration

bottom ash (MSWIBA) replace natural aggregates on the mechanical, microscopic and environmental properties, durability of sustainable concrete, J. Clean. Prod. 337 (2022) 130479, https://doi.org/10.1016/J.JCLEPRO.2022.130479.
[28] J. Bao, R. Zheng, P. Zhang, Y. Cui, S. Xue, Q. Song, Y. Ma, Thermal resistance, water absorption and microstructure of high-strength self-compacting lightweight aggregate concrete (HSSC-LWAC) after exposure to elevated temperatures, Construct. Build. Mater. 365 (2023) 130071, https://doi.org/10.1016/J.CONBUILDMAT.2022.130071.
[29] T. Lim, J.H. Lee, J.H. Mun, K.H. Yang, S. Ju, S.M. Jeong, Enhancing functionality of epoxy–TiO2-embedded high-strength lightweight aggregates, Polymers 12 (2020) 1–11, https://doi.org/10.3390/polym12102384.
[30] J. Liu, C. Shi, N. Farzadnia, X. Ma, Effects of pretreated fine lightweight aggregate on shrinkage and pore structure of ultra-high strength concrete, Construct. Build. Mater. 204 (2019) 276–287, https://doi.org/10.1016/J.CONBUILDMAT.2019.01.205.
[31] K.S. Youm, J. Moon, J.Y. Cho, J.J. Kim, Experimental study on strength and durability of lightweight aggregate concrete containing silica fume, Construct. Build. Mater. 114 (2016) 517–527, https://doi.org/10.1016/j.conbuildmat.2016.03.165.
[32] J. Jiang, J. Qin, H. Chu, Improving mechanical properties and microstructure of ultra-high-performance lightweight concrete via graphene oxide, J. Build. Eng. 80 (2023) 108038, https://doi.org/10.1016/J.JOBE.2023.108038.
[33] H. Chu, J. Qin, L. Gao, J. Jiang, F. Wang, L. Wang, A cost-effective approach to manufacturing ultra-high-performance lightweight concrete via air-entraining, Arch. Civ. Mech. Eng. 23 (2023) 1–19, https://doi.org/10.1007/S43452-023-00751-2/FIGURES/19.
[34] E. Güneyisi, M. Gesoglu, H. Ghanim, S. Ipek, I. Taha, Influence of the artificial lightweight aggregate on fresh properties and compressive strength of the self-compacting mortars, Construct. Build. Mater. 116 (2016) 151–158, https://doi.org/10.1016/J.CONBUILDMAT.2016.04.140.
[35] Q. Wang, H. Chu, W. Shi, J. Jiang, F. Wang, Feasibility of preparing self-compacting mortar via municipal solid waste incineration bottom ash: an experimental study, Arch. Civ. Mech. Eng. 23 (2023) 1–16, https://doi.org/10.1007/S43452-023-00794-5/FIGURES/17.
[36] H. Chu, Q. Wang, W. Zhang, Optimizing ecological ultra-high performance concrete prepared with incineration bottom ash: utilization of Al2O3 micro powder for improved mechanical properties and durability, Construct. Build. Mater. 426 (2024) 136152, https://doi.org/10.1016/J.CONBUILDMAT.2024.136152.
[37] Q. Wang, H. Chu, J. Jiang, B. Zhu, Enhancing mechanical performance and durability of high strength mortar with incineration bottom ash via Al2O3 micro-powder: an experimental study, J. Build. Eng. 89 (2024) 109268, https://doi.org/10.1016/J.JOBE.2024.109268.
[38] S. Bozorgmehr Nia, M. Nemati Chari, Applied development of sustainable-durable high-performance lightweight concrete: toward low carbon footprint, durability, and energy saving, Results Mater 20 (2023) 100482, https://doi.org/10.1016/J.RINMA.2023.100482.
[39] Q. Zhao, Y. Shi, C. Xue, Y. Jia, W. Guo, D. Wang, S. Wang, Y. Gao, Investigation of various curing methods on the properties of red mud-calcium carbide slag-based artificial lightweight aggregate ceramsite fabricated through alkali-activated cold-bonded pelletization technology, Construct. Build. Mater. 401 (2023) 132956, https://doi.org/10.1016/J.CONBUILDMAT.2023.132956.
[40] ASTM C39/39M, Standard test method for compressive strength of cylindrical concrete specimens, Annu. Book ASTM Stand. i (2021) 1–8. https://www.astm.org/c0039_c0039m-21.html. (Accessed 7 January 2023).
[41] ASTM C496, Standard test method for splitting tensile strength, Annu. Book ASTM Stand. i (2017) 1–4, https://doi.org/10.1520/C0496.
[42] P.K. Dehdezi, S. Erdem, M.A. Blankson, Physico-mechanical, microstructural and dynamic properties of newly developed artificial fly ash based lightweight aggregate – rubber concrete composite, Composites, Part B 79 (2015) 451–455, https://doi.org/10.1016/J.COMPOSITESB.2015.05.005.
[43] O. Aungatichart, N. Nawaukkaratharnant, T. Wasanapiarnpong, The potential use of cold-bonded lightweight aggregate derived from various types of biomass fly ash for preparation of lightweight concrete, Mater. Lett. 327 (2022) 133019, https://doi.org/10.1016/J.MATLET.2022.133019.
[44] X. Yang, C. Jin, T. Liu, J. Jiang, N. Mao, J. Huang, Y. Wu, Z. Lu, J. Li, Effect of brick-based construction and demolition waste on the performance and microstructure of lightweight aggregate concrete, J. Build. Eng. 78 (2023) 107665, https://doi.org/10.1016/J.JOBE.2023.107665.
[45] Y. Zhang, X. Sun, An investigation of the hybrid effect of pre-absorbed lightweight aggregate and basalt-polypropylene fiber on concrete performance, Construct. Build. Mater. 408 (2023) 133626, https://doi.org/10.1016/J.CONBUILDMAT.2023.133626.
[46] P. Kumar, D. Pasla, T. Jothi Saravanan, Self-compacting lightweight aggregate concrete and its properties: a review, Construct. Build. Mater. 375 (2023) 130861, https://doi.org/10.1016/J.CONBUILDMAT.2023.130861.
[47] T. Haller, N. Beuntner, H. Gutsch, K.C. Thienel, Challenges on pumping infra-lightweight concrete based on highly porous aggregates, J. Build. Eng. 65 (2023) 105761, https://doi.org/10.1016/J.JOBE.2022.105761.
[48] M.L. Abbas, W.A. Abbas, E. Güneyisi, Shrinkage and thermo-mechanical properties of concretes incorporated with different substitutions of natural aggregates by cold bonded calcined attapulgite lightweight aggregates, J. Build. Eng. 79 (2023) 107921, https://doi.org/10.1016/J.JOBE.2023.107921.
[49] A. Benli, Mechanical and durability properties of self-compacting mortars containing binary and ternary mixes of fly ash and silica fume, Struct. Concr. 20 (2019) 1096–1108, https://doi.org/10.1002/SUCO.201800302.
[50] J. Wang, P. Hu, Y. Liu, Z. Qian, C. Hu, H. Zhang, Axial compressive behavior of the PEC slender columns with lightweight aggregate concrete, J. Constr. Steel Res. 211 (2023) 108206, https://doi.org/10.1016/J.JCSR.2023.108206.
[51] M. Maghfouri, V. Alimohammadi, R. Gupta, M. Saberian, P. Azarsa, M. Hashemi, I. Asadi, R. Roychand, Drying shrinkage properties of expanded polystyrene (EPS) lightweight aggregate concrete: a review, Case Stud. Constr. Mater. 16 (2022) e00919, https://doi.org/10.1016/J.CSCM.2022.E00919.
[52] N. Arioglu, Z. Canan Girgin, E. Arioglu, Evaluation of ratio between splitting tensile strength and compressive strength for concretes up to 120 MPa and its application in strength criterion, Materials J. 103 (2006) 18–24, https://doi.org/10.14359/15123.
[53] P. Alexandrina De Aguiar, P. Marques, X. Hong, J.C. Lee, B. Qian, Mechanical properties and microstructure of high-strength lightweight concrete incorporating graphene oxide, Nanomaterials 12 (2022) 833 https://doi.org/10.3390/NANO12050833, 12 (2022) 833.
[54] Z. Bian, Y. Huang, J.X. Lu, G. Ou, S. Yang, C.S. Poon, Development of self-foaming cold-bonded lightweight aggregates from waste glass powder and incineration bottom ash for lightweight concrete, J. Clean. Prod. 428 (2023) 139424, https://doi.org/10.1016/J.JCLEPRO.2023.139424.
[55] H.A. Mahmoud, T.A. Tawfik, M.M. Abd El-razik, A.S. Faried, Mechanical and acoustic absorption properties of lightweight fly ash/slag-based geopolymer concrete with various aggregates, Ceram. Int. 49 (2023) 21142–21154, https://doi.org/10.1016/J.CERAMINT.2023.03.244.